ARTICLE

Otud7a Knockout Mice Recapitulate Many Neurological Features of 15q13.3 Microdeletion Syndrome

Jiani Yin,[1,2] Wu Chen,[3,4,10] Eugene S. Chao,[3,4,10] Sirena Soriano,[1,2,10] Li Wang,[1,2,10] Wei Wang,[1,2] Steven E. Cummock,[2] Huifang Tao,[1,2] Kaifang Pang,[2,6] Zhandong Liu,[2,6] Fred A. Pereira,[8,9] Rodney C. Samaco,[1,2,5] Huda Y. Zoghbi,[1,2,7] Mingshan Xue,[1,3,4] and Christian P. Schaaf[1,2,*]

15q13.3 microdeletion syndrome is characterized by a wide spectrum of neurodevelopmental disorders, including developmental delay, intellectual disability, epilepsy, language impairment, abnormal behaviors, neuropsychiatric disorders, and hypotonia. This syndrome is caused by a deletion on chromosome 15q, which typically encompasses six genes. Here, through studies on OTU deubiquitinase 7A (*Otud7a*) knockout mice, we identify *OTUD7A* as a critical gene responsible for many of the cardinal phenotypes associated with 15q13.3 microdeletion syndrome. *Otud7a*-null mice show reduced body weight, developmental delay, abnormal electroencephalography patterns and seizures, reduced ultrasonic vocalizations, decreased grip strength, impaired motor learning/motor coordination, and reduced acoustic startle. We show that OTUD7A localizes to dendritic spines and that *Otud7a*-null mice have decreased dendritic spine density compared to their wild-type littermates. Furthermore, frequency of miniature excitatory postsynaptic currents (mEPSCs) is reduced in the frontal cortex of *Otud7a*-null mice, suggesting a role of Otud7a in regulation of dendritic spine density and glutamatergic synaptic transmission. Taken together, our results suggest decreased *OTUD7A* dosage as a major contributor to the neurodevelopmental phenotypes associated with 15q13.3 microdeletion syndrome, through the misregulation of dendritic spine density and activity.

Introduction

The proximal part of chromosome 15 long (q) arm is one of the most unstable regions of the human genome, largely due to six low copy repeat (LCR) elements, which are likely to mediate non-allelic homologous recombination (NAHR). These LCR elements often become breakpoints in chromosomal rearrangements and are named breakpoints BP1–BP6.

Chromosomal deletions and duplications are frequently associated with disease. 15q13.3 microdeletions were first described in 2008 as a rare condition associated with intellectual disability and seizures.[1] Current estimate of the frequency of 15q13.3 microdeletion in the general population is 1 in 30,000 to 40,000 individuals, with some sources reporting an even higher frequency.[1–4] Further assessment of clinical implications of 15q13.3 microdeletion suggests that some individuals who carry the deletion may be unaffected, whereas others manifest a wide spectrum of neuropsychiatric symptoms.[2,5,6] Statistically, 55%–75% of affected individuals show developmental delay or cognitive deficits. Seizures or EEG abnormalities have been reported in about one third of individuals (28%–42%). Language impairment and dysmorphic features are often seen (16%–30%). About 10% of individuals meet formal criteria for autism spectrum disorder (MIM: 209850). Finally, a subset of individuals have attention deficit hyperactivity disorder (ADHD), mood disorders, aggression, schizophrenia, and/or hypotonia.[7] Please refer to Lowther et al. for a schematic view of heterozygous and homozygous 15q13.3 microdeletions and a review of the human case subjects.[6]

The 15q13.3 microdeletions commonly encompass six protein-coding genes: *FAN1* (MIM: 614817), *MTMR10*, *TRPM1* (MIM: 603576), *KLF13* (MIM: 605328), *OTUD7A* (MIM: 612024), and *CHRNA7* (MIM: 118511). Smaller deletions that involve only one exon of *OTUD7A* and the entire *CHRNA7* have been found in individuals who manifest phenotypes similar to affected individuals with larger deletions.[5,8] *CHRNA7*, which encodes for a nicotinic receptor, has been considered as the major candidate gene to account for the neurological phenotypes of 15q13.3 microdeletion syndrome (MIM: 612001). However, our recent work showed that mice deficient in *Chrna7* do not recapitulate the cognitive, behavioral, or electrophysiological phenotypes seen in human individuals,[9] which raises the possibility that *OTUD7A* may account for the phenotypes associated with 15q13.3 microdeletion syndrome.

[1]Department of Molecular and Human Genetics, Baylor College of Medicine, Houston, TX, USA; [2]Jan and Dan Duncan Neurological Research Institute, Texas Children's Hospital, Houston, TX, USA; [3]Department of Neuroscience, Baylor College of Medicine, Houston, TX, USA; [4]The Cain Foundation Laboratories, Jan and Dan Duncan Neurological Research Institute, Texas Children's Hospital, Houston, TX, USA; [5]Program in Translational Biology and Molecular Medicine, Baylor College of Medicine, Houston, TX, USA; [6]Department of Pediatrics, Baylor College of Medicine, Houston, TX, USA; [7]Howard Hughes Medical Institute, Baylor College of Medicine, Houston, TX, USA; [8]Huffington Center on Aging and Department of Molecular and Cellular Biology, Baylor College of Medicine, Houston, TX 77030, USA; [9]Bobby R. Alford Department of Otolaryngology-Head and Neck Surgery, Baylor College of Medicine, Houston, TX 77030, USA
[10]These authors contributed equally to this work
*Correspondence: schaaf@bcm.edu
https://doi.org/10.1016/j.ajhg.2018.01.005.

Material and Methods

sgRNA and Cas9 Preparation

Donor DNAs expressing sgRNAs under the T7 promoter were prepared by PCR, using Phusion High-Fidelity polymerase (New England Biolabs), pX330 as a template, and a combination of reverse primer with one of two forward primers: forward primer for exon 4 of *OTUD7A* 5′-TTAATACGACTCACTATAGGCTAGCGAGGCGGCATGTAAGGTTTTAGAGCTAGAAATAGC-3′, forward primer for exon 6 of *OTUD7A* 5′-TTAATACGACTCACTATAGGGAAGTGTGTGCGAGGCTCGCGTTTTAGAGCTAGAAATAGC-3′, reverse primer 5′-AAAAGCACCGACTCGGTGCC-3′.

The resulting PCR products were subjected to RNA transcription, using the MEGAshortscript T7 Transcription kit (Thermo Fisher Scientific) with manufacturer's protocol. The sgRNAs were purified by the MEGAshortscript Transcription Clean-Up kit (Thermo Fisher Scientific).

Cas9 was ordered from PNA TECHNOLOGY and stored at −80°C. On the day of microinjection, final concentrations of 30 ng/μL Cas9 and 20 ng/μL sgRNA (total) were mixed into a 150 μL injection buffer (10 mM Tris [pH 7.5], 0.25 mM EDTA) and heated at 37°C for 5 min. After centrifuging at 20,000 × *g* for 10 min at 4°C, the top 2/3 of supernatant was used for cytoplasmic microinjection.

Cytoplasmic Microinjection

C57BL/6J female mice were superovulated and mated with C57BL/6J males, and fertilized eggs were collected from the oviduct. The pronuclear-stage eggs were injected with Cas9 and sgRNAs at the indicated concentrations. The eggs were cultivated in kSOM overnight and then transferred into the oviducts of pseudopregnant FVB females.

Genotyping

The last 1–2 mm of mouse tails were cut into a 1.5 mL Eppendoff tube containing 135 μL 50 mM NaOH and incubated overnight on a 55°C shaker. DNAs were extracted by adding 15 μL Tris-HCL at pH 6.8, and centrifuging at 20,000 × *g* for 1 min.

1 μL of DNA was used for each PCR reaction using Econo taq DNA polymerase (Lucigen, WI). Forward primer for wild-type 5′-TCATGAACCAGCTTCCCTTT-3′, reverse primer for wild-type 5′-GCTAGCATGCAGGGTCACTT-3′, forward primer for mutant 5′-TGTGCACGAGCTGTAAAAGG-3′, reverse primer for mutant 5′-GTGGCAACAACCACTGTCAC-3′. To genotype off-target candidates, primers in Table S1 were used.

Plasmid Preparation

To construct pCMV-3xFLAG-OTUD7A plasmid, human OTUD7A coding regions were PCR amplified and placed into the pCMV10-3xFLAG plasmid between multicloning sites HindIII and XbaI. To construct a pCMV6-OTUD7A-MYC-FLAG, human OTUD7A coding regions together with MYC were PCR amplified from a Myc-DDK-tagged OTUD7A plasmid (Origene Ca. #RC213015) and placed into a pCMV6-FLAG plasmid.

Animals

Mice were maintained on a 14 hr light/10 hr dark cycle, with access to regular mouse chow and water *ad libitum*. For behavioral assessments, heterozygous founders from CRISPR/Cas9 microinjection were backcrossed to wild-type mice (C57BL/6J) for two generations to obtain heterozygous mice for breeding pairs. All of the *Otud7a* homozygous (KO) and heterozygous (HET) mutant mice as well as the wild-type (WT) mice used in our experiments were derived from HET breeding pairs. Mice were randomly assigned and group-housed, with two to five animals per cage, immediately after weaning. Cohort one, consisting of 21 WT, 27 HET, and 15 KO mice, with mixed sex, were monitored for developmental phenotypes. Mice for ultrasonic vocalization recordings (cohort two) consist of 16 WT, 29 HET, and 19 KO mice, with mixed sex. Cohort three, consisting of 14 WT (♂), 20 HET (♂), 14 KO (♂), 14 WT (♀), 20 HET (♀), and 16 KO (♀) mice, went through a series of assays, including elevated plus maze, open field activity, light-dark activity, self-grooming, holeboard exploration, rotarod test, three-chamber test, partition test, forced swimming test, prepulse inhibition, conditioned fear, and nest building, all of which started at 10 weeks of age. Cohort four, consisting of 13 WT (♂), 19 HET (♂), 14 KO (♂), 19 WT (♀), 18 HET (♀), and 13 KO (♀) mice, were monitored for body weight and tested in grip strength and novel object recognition. Experiments were performed during the light cycle, and mice were given inter-test intervals of 1–2 days between each test. All behavioral tests were performed at 700–750 lux illumination and background white noise at approximately 60 dB, with the exception of the partition test, in which there was no background white noise.

For all assays, the experimenter remained blind to the genotypes. All research and animal care procedures were approved by the Baylor College of Medicine Animal Care and Use Committee and were performed in accordance with the relevant guidelines and regulations. The *Otud7a*-null mouse line will be available from The Jackson Laboratory as JAX#031294.

Developmental Assessment

Neurobehavioral development was examined during the preweaning period, using a battery of tests that evaluated sensorial and motor responses reflecting the maturation of the CNS, as described previously.[10] The day of appearance of developmental landmarks, including negative geotaxis, cliff aversion, incisor eruption and growth, eye lid opening, and ear opening, was recorded. To evaluate negative geotaxis, pups were placed facedown on a paper box that was tilted 30° from the horizon line. The day when the pup turned around to face upward was recorded. To evaluate cliff aversion, pups were placed with their legs just within the edge of a paper box. The day when the pup avoided falling off the edge was recorded. Incisor growth was evaluated by the appearance of shiny spots at the tip of the incisors.

Ultrasonic Vocalization

Ultrasonic vocalization was recorded on postnatal days 2, 4, 6, 8, and 10. All recordings were performed between 10:00 AM and 4:00 PM. On the first day of recording, the subjects were marked for identification by Sharpie pen on tails or backs, immediately following the recording. On the following days, subjects were re-marked in the same way immediately after recording. On day 10, subjects were ear tagged and the last 1–2 mm of tail was clipped for genotyping. At the time of recording, a litter was separated from its parents and placed in an empty clean cage with beddings heated to 37°C on a heat mat. Temperature at the top of the bedding was monitored with a forehead digital thermometer (BARUN, MA). For each recording, a pup was moved with minimal handling into a cup, which was placed into an anechoic, sound-attenuating chamber (Med Associates Inc.). The pup was then allowed to rest for 1–2 min. Subsequently, audio was recorded

for 2 min using a CM16 microphone (Avisoft Bioacoustics) and amplified/digitized using UltraSoundGate 416H, at a 250 kHz sampling rate and a bit depth of 16, using Avisoft RECORDER software.

Rotarod Test

Motor coordination and motor learning was assessed, using an accelerating rotarod (UGO Basile). Mice at 11 weeks of age were placed on the rotating drum, which accelerated from 4 to 40 rpm over a 5 min period. Time spent walking on top of the rod before falling off was recorded manually, with a maximum time of 5 min. Mice were given four trials per day over 4 consecutive days, with an inter-trial rest interval of more than 30 min.

Prepulse Inhibition

The prepulse inhibition (PPI) was used to evaluate schizophrenia-associated behavior at 13 weeks of age, as described previously.[9] Mice were placed into startle chambers (SR-LAB, San Diego Instruments). The prepulse+pulse trials consisted of a 20 ms prepulse sound, a 100 ms delay, followed by a 40 ms 120 dB startle pulse. Prepulse intensities were 74, 78, and 82 dB. The NOSTIM trial consisted of background noise only. Each trial type was presented six times, in pseudorandom order, with an inter-trial interval of 10 to 20 s. Percent prepulse inhibition of the startle response was calculated for each acoustic prepulse intensity as 100 – [(startle response on the prepulse plus startle stimulus /startle response alone) × 100].

Grip Strength

Grip strength was measured at 25 weeks of age. Each mouse was held by the tail and allowed to grasp the middle of the bar of the Chatillon-Ametek grip strength meter (Columbus Instruments) with both of its forepaws. Then the mouse was pulled away from the bar until it released it, and the maximum force generated was recorded. The test was repeated three times for each mouse, and the grip strength values were acquired by averaging the scores from the three pulls.

Behavioral Data Analysis and Statistics

Statistical analysis of genotype and sex effects on behavioral studies were performed using Kruskal-Wallis test, two-, or three-way analysis of variance (ANOVA). If a Kruskal-Wallis test was significant, Dunn's multiple comparison test was performed for between-group comparisons. If an ANOVA was significant, a Tukey's HSD post hoc test or post hoc interaction analysis was performed for between-group comparisons or interaction analysis. Detailed statistical analysis for behavioral data was provided in Table S3. p values of < 0.05 were considered to be statistically significant. All data were presented as mean ± SEM (GraphPad Prism 6.0e).

Surgery and EEG Recordings

Video EEG and EMGs were acquired from three WT (♂), three KO (♂), three WT (♀), and three KO (♀) animals at 4 months of age. The methods were modified from previous publications.[12] Adult mice at 14 weeks were anesthetized with 1%–2% isoflurane. Under aseptic conditions, each mouse was surgically implanted with the cortical EEG recording electrodes (Teflon-coated silver wire, 127 μm diameter) in the subdural space of the left frontal cortex and the right parietal cortex, respectively, with the reference electrode positioned in the occipital region of the skull. The third recording electrode (Teflon-coated tungsten wire, 50 μm diameter) was aimed at the dentate gyrus (P2.0R1.8H1.8), with the reference electrode at the corpus callosum. In addition, the fourth recording electrode (silver wire) was inserted into the neck muscles, to monitor the electromyogram (EMG) as an indicator of animal activity level. All electrode wires were attached to a miniature connector (Harwin Connector) and secured on the skull by dental cement. After 2 weeks of post-surgical recovery, simultaneous EEG activity, EMG activity (filtered between 0.1 Hz and 1 kHz, sampled at 2 kHz), and behavior were recorded in freely moving mice for 2 hr per day over a 4 day span.

EEG Data Analysis

EEG data were processed by custom-written algorithms in MATLAB R2015b. Briefly, EEG signals were divided into 10-min segments and each segment was filtered with a third order Butterworth bandpass filter (0.5 and 400 Hz cutoffs). To identify seizure-like events, the filtered data were divided into 500-ms non-overlapping epochs. EEG changes that occurred in the time domain were captured by amplitude correlation (autocorrelation value between successive epochs) and root mean square (average amplitude of the epoch). Changes that occurred in the frequency domain were captured by frequency band ratio, where the power of the upper band (100–300 Hz) was contrasted with that of the lower band (0.5–80 Hz). An EEG segment that exceeded the thresholds for all three of the above quantitative features was identified as a candidate for epileptiform activity. Each candidate and the corresponding video were then visually inspected to confirm as a seizure-like event. For each seizure-like event, the duration (the time difference between the first and last peaks), spike amplitude (the average amplitude of spike peaks), and spike frequency were quantified. To identify repetitive-spike events, the filtered data were divided into 250-ms non-overlapping epochs, and frequency band ratio (0.5–80 Hz for the lower band and 100–300 Hz for the upper band), root mean square, and spike density (number of spikes per epoch) were used. An EEG segment that exceeded the thresholds for all three of the above quantitative features was identified as a candidate and was then visually inspected to confirm as a repetitive-spike event. Data were analyzed blindly to the genotypes.

Primary Neuronal Culture and Transfection

2% B-27 supplement (Life Technology, Ca. 17504-044), 1× GlutaMAX supplement (Life Technology, Ca. 35050-061), and 1× penicillin-streptomycin (Life Technology, Ca. 15140-122), were added to Neurobasal Medium (Thermo Fisher, 21103-049) to make complete Neurobasal Medium for primary cortical neuronal culture. Cortices, together with hippocampi, were dissected out from wild-type and knockout postnatal day 0 pups using sterile dissection tools, and meninges were carefully removed. The last 1–2 mm of their tails were used for genotyping. The cortices from each mouse were placed into 500 μL complete Neurobasal Medium with 10% Fetal Bovine Serum (Thermo Fisher Scientific, Ca. 10439016) in an eppendoff tube, on a 37°C heat block, shaking at 1,000 rpm. After dissection was performed for all mice, tubes were taken out of the shaker to let the tissue settle. Next, supernatants were removed, and tissues were allowed to incubate in 500 μL preheated papain solution from the Papain kit (Worthington Biochemical Corp, Ca. LK003150) on the 37°C shaker for 45 min. Then, supernatants were removed and tissues were triturated rigorously in preheated 500 μL complete

Neurobasal Medium with 1 mL pipette, until no clumps of cell were visible (about 25 times of pipetting up and down). The number of cells was quantified and 1 million cells were plated in complete Neurobasal Medium with 10% Fetal Bovine Serum (FBS) on poly-D-lysine/laminine pre-coated coverslips (Fisher Scientific, Ca. 08-774-385) in 24-well plates. Half of the media was changed with complete Neurobasal medium without FBS on the following day, and then was changed every 3 days until DIV 14 for immunofluorescence.

Primary neurons were transfected with plasmids on DIV 7, using Lipofectamine 2000 (Thermo Fisher, Ca. 11668-019). 300 ng of pEGFP-C1 (Clontech) and 700 ng of pcDNA3 or plasmid that expresses OTUD7A were mixed with 100 μL Neurobasal Medium and 2 μL Lipofectamine 2000, and incubated for 30 min at room temperature. 20 min after incubation, we collected the conditioned media from the primary neuronal cultures and replaced them with 1 mL pre-warmed Neurobasal Medium (without any supplement). When the 30 min incubation time was complete, we added 400 μL of pre-warmed Neurobasal Medium to the 100 μL mixture and changed the media of each well to this 500 μL new mixture. Each well was washed twice with 800 μL Neurobasal Medium after 3–4 hr of incubation at 37°C and was replaced back to the collected conditioned media. Primary neuronal culture and measurement of dendritic spine density have been repeated three times. Spines were quantified from secondary apical dendrites, and the experimenter remained blind to the genotypes. The four spine categories were identified by the same criteria as the following reference.[13]

Immunofluorescence

Immunofluorescence assay was done on DIV 14 in mouse primary neuronal cultures, 24–48 hr after transfection in HeLa cells. Cells were rinsed with 1× PBS once and then fixed with 10% Formalin for 10 min at room temperature. After three cycles of washing with 1× PBS, cells were permeabilized and blocked in 0.1% triton and 2% donkey serum for 30 min. Cells were then incubated with primary antibodies: mouse anti-FLAG (Sigma, Ca. F1804) and chicken anti-GFP (Abcam, ab13970), at 4°C overnight. After three cycles of washing with 1× PBS, cells were incubated with donkey anti-chicken Alexa488 or anti-mouse Cy3 (Thermo Fisher) secondary antibodies at 1:500, for 1 hr at room temperature. After three cycles of washing with 1× PBS, cells were mounted in mounting medium containing DAPI and imaged with a confocal microscope (Zeiss 880) on the following days.

Golgi-Cox Staining

Three WT and three KO female mice at 4 weeks of age were used. Animals were deeply anesthetized and brains were removed. Golgi-Cox staining was performed using an FD Rapid GolgiStain Kit (FD NeuroTechnologies) according to the manufacturer's instructions. The coronal brain blocks were immersed in a solution of equal parts solutions A and B at room temperature for 2 weeks and then soaked in solution C at 4°C for 48 hr. After freezing with isopentane and embedding in OCT medium, the brain samples were sliced into 50 μm pieces at −22°C using a cryostat microtome. Each frozen section was mounted with solution C on a 0.5% gelatin-coated glass slide. Slides were allowed to dry naturally at room temperature and were then stained with a mixture (solution D: solution E: DW; 1:1:2) for 5 min, after which the slides were rinsed in distilled water twice for 4 min each. Slides were dehydrated in an ascending ethanol series and then sealed with cytoseal (Thermo Fisher Scientific) through xylene.

Bright-field images of basal dendrites of pyramidal neurons from frontal association cortex (FrA), motor cortex (M1/M2), and somatosensory cortex (S1/S2) were acquired using a confocal microscope (Zeiss 880) with z stacks. Dendritic spines were manually counted (from 20 WT FrA, 16 WT M1/M2, 19 WT S1/S2, 19 KO FrA, 18 KO M1/M2, 18 KO S1/S2 dendrites) by an experimenter who was blind to the genotypes, and statistical analysis was performed using two-way ANOVA followed by Bonferroni's multiple comparisons test.

Frontal Cortical Slice Electrophysiology

Acute fresh coronal slices (350 μm thick) containing frontal cortex were prepared from 8- to 11-week-old mice with a vibratome slicer (Leica Microsystems). Acute slices were collected in chilled (2°C–5°C) cutting solution containing (in mM) 110 choline-chloride, 25 $NaHCO_3$, 25 D-glucose, 11.6 sodium ascorbate, 7 $MgSO_4$, 3.1 sodium pyruvate, 2.5 KCl, 1.25 NaH_2PO_4, and 0.5 $CaCl_2$. Then, slices were incubated in standard artificial cerebrospinal fluid (ACSF, in mM) containing 119 NaCl, 26.2 $NaHCO_3$, 11 D-glucose, 3 KCl, 2 $CaCl_2$, 1 $MgSO_4$, and 1.25 NaH_2PO_4 at 37°C for 30 min before being stored at room temperature for recording. All solutions were saturated with 95% O_2 and 5% CO_2.

Whole-cell recordings were made from visually identified pyramidal neurons in layer 2/3 regions of frontal cortices by using a patch clamp amplifier (MultiClamp 700 B, Molecular Devices). Microelectrodes with resistance of 2–3 MΩ were pulled from borosilicate glass capillaries (Sutter Instruments). The intrapipette solution for recording mEPSC (holding at −70 mV) contained (in mM) 140 potassium gluconate, 5 KCl, 10 HEPES, 0.2 EGTA, 2 $MgCl_2$, 4 MgATP, 0.3 Na_2GTP, and 10 Na2-phosphocreatine (pH 7.2). Picrotoxin (100 μM), D-2-amino-5-phosphonopentanoic acid (AP5, 50 μM), and Tetrodotoxin (TTX, 0.1 μM) were present in the ACSF for mEPSC recording.

The whole-cell recording was performed at (30°C ± 1°C) by using an automatic temperature controller (Warner Instrument). Data acquisition was performed by using a digitizer (DigiData 1440A, Molecular Devices). Minianalysis 6.0.7 (Synaptosoft Inc) and pClamp 10 (Molecular Devices) were used for data analysis. Data were discarded when the resistance change was greater than 20% during the course of the experiment. Data are shown as mean ± standard error of mean and analyzed by Mann-Whitney test.

Results

Generation of *Otud7a* Knockout Mice

Given that the smallest deletion found in individuals with 15q13.3 microdeletion syndrome removes *CHRNA7* and part of *OTUD7A*[5] and that *OTUD7A* is mainly expressed in the central nervous system (GTEx database), we set out to generate a knockout mouse model of *Otud7a*. We designed two sgRNAs that delete most of the OTU deubiquitinase domain, which created a premature stop codon in exon 8. Using cytoplasmic microinjection of the sgRNAs, along with Cas9 into 1-cell stage C57BL/6J embryos (Figure 1), we obtained deletions at the desired locus and of the expected size. These deletions were validated by tail DNA sequencing of founder mice and their offspring (Figure 1). No off-target mutations were found

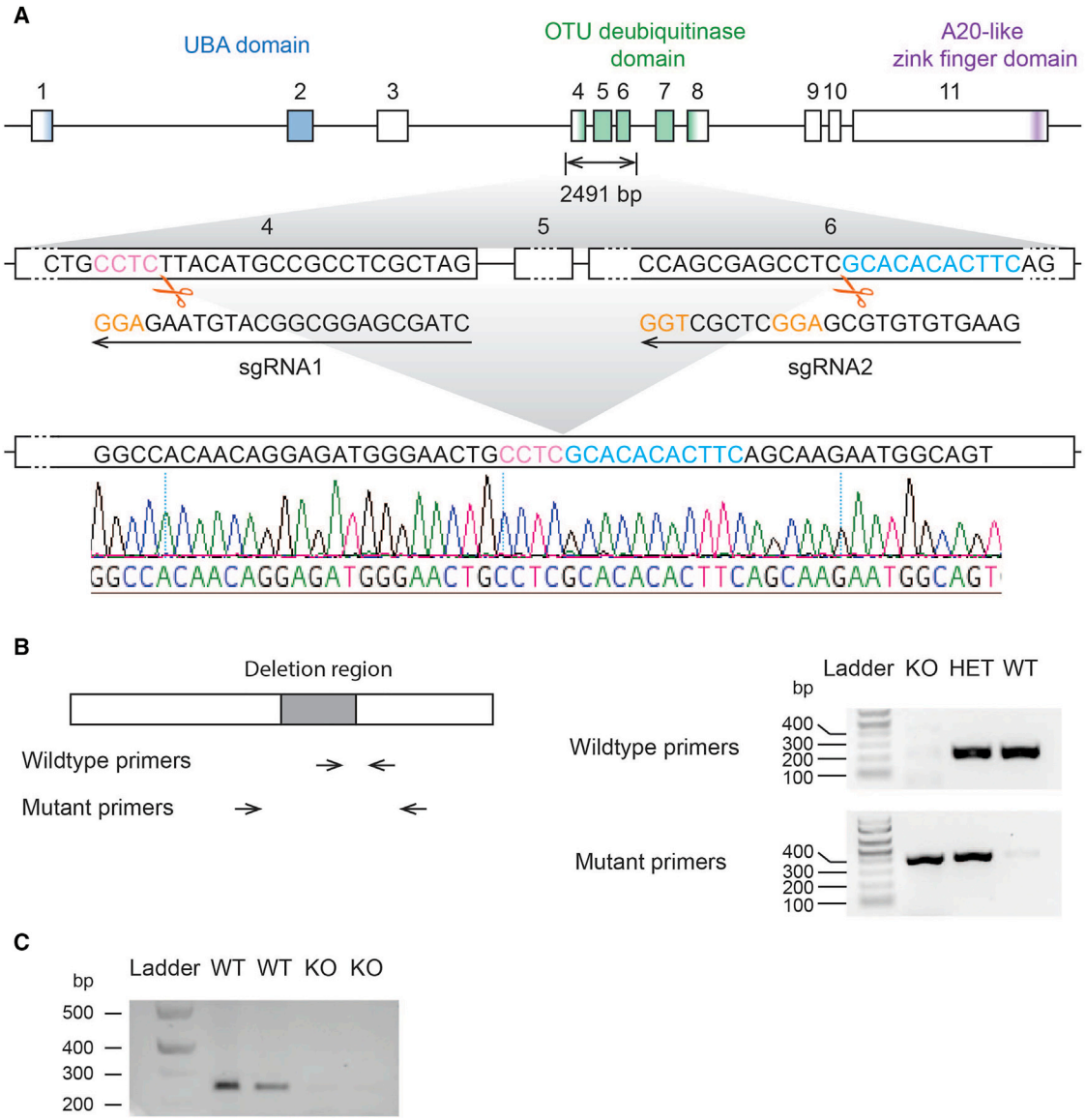

Figure 1. Generation of the *Otud7a* Knockout Mouse Model

(A) Scheme of *Otud7a* knockout design and sequencing validation. Exons of *Otud7a* are boxed, whereas introns are represented by lines in between exons. All exons and introns are plotted in scale within their category. Three domains have been identified in OTUD7A: the UBA domain, OTU deubiquitinase, and an A20-like zinc finger domain. The nucleotides encoding these domains are colored blue, green, and purple, respectively. NGG sequences in the two sgRNAs are shown in orange. Following CRISPR/Cas9 manipulation, we obtained mice with knockout of the expected region, bordering sequences of which are highlighted in pink and blue. Sequencing trace from tail DNA of the mice are shown at the bottom.

(B) Genotype identification of *OTUD7A*-deficient mice. The knockout region was boxed in gray. Genotyping primer binding regions for wild-type and knockout primer sets were indicated by arrows. In the representative genotyping results, animals that carry a wild-type allele show bands at 223 bp with wild-type primers, and those that carry a knockout allele show bands at 389 bp with mutant primers.

(C) RT-PCR products with RNA extracted from brains of wild-type and *Otud7a* knockout mice showing a deficiency of *Otud7a* transcripts in the knockout animals. Primers used for RT-PCR bind to exon 3 and 8 respectively. Forward primer: 5′-GGACTTCAGGAGCTTCATCG-3′, reverse primer: 5′-ACCTCCAAGGGCAGGTAGAT-3′. Expected PCR product size is 244 bp.

by sequencing the top 15 off-target candidates for each sgRNA predicted by CRISPR design tool (Table S1).

Behavioral and Electroencephalographical Abnormalities in *Otud7a* Knockout Mice

In an attempt to address whether *Otud7a* has an effect on phenotypes in close relation to 15q13.3 microdeletion syndrome, we compared *Otud7a* homozygous and heterozygous knockout mice with wild-type littermates, using a battery of 16 behavioral paradigms and electroencephalography (EEG)/electromyography (EMG) recordings (Table 1). Although there was little difference in disease expression between male and female affected individuals, we performed all behavioral and electrophysiological assays on both male and female *Otud7a* knockout mice.

Table 1. Behavioral Assays Used in Correlation to Clinical Manifestations of 15q13.3 Microdeletion Patients

Patient Phenotype	Behavioral Test	Cohort	Age (weeks)
Developmental delay	developmental milestones	1	0–2
Language impairment	ultrasonic vocalization	2	0–1.5
Intellectual disability	conditioned fear	3	13
	novel object recognition	4	27
Motor deficits	rotarod	3	11
Schizophrenia	prepulse inhibition	3	13
Autism (social interaction deficits)	three-chamber test	3	12
	partition test	3	12
	nest building	3	14
Autism (repetitve behaviors)	self-grooming	3	10
	holeboard exploration	3	10
Hypotonia	grip strength	4	25
Anxiety	elevated plus maze	3	10
	light-dark box exploration	3	10
Hyperactivity	open field activity	3	10
Depression	forced swimming test	3	12

Cohort 1: 21 WT, 27 HET, and 15 KO
Cohort 2: 16 WT, 29 HET, and 19 KO
Cohort 3: 14 WT (♂), 20 HET (♂), 14 KO (♂), 14 WT (♀), 20 HET (♀), and 16 KO (♀)
Cohort 4: 15 WT (♂), 18 HET (♂), 19 KO (♂), 18 WT (♀), 15 HET (♀), and 16 KO (♀)

Developmental delay and intellectual disability are the most prevalent phenotypes (50%–60%) seen in individuals with 15q13.3 microdeletions.[7] We therefore assessed development in our *Otud7a* mutant mouse model. We found that *Otud7a* homozygous null mice presented a significant preweaning growth delay, as they had a 30% weight reduction compared to heterozygous knockout or wild-type littermates (Figure 2A). This finding is in accordance with the fact that five out of seven individuals with 15q13.3 homozygous microdeletions reported growth rates below 3rd percentile at 9–10 years of age.[3,4,14–16] The overall brain structure and organization in homozygous null mice appears normal (data not shown). To further evaluate the neurobehavioral development of *Otud7a* mice, we monitored pups of different genotypes every day, from postnatal day 0 to 14, and recorded the day on which they reached various developmental milestones. These milestones included negative geotaxis, cliff aversion, incisor eruption/growth, eye lid opening, and ear opening. We found that *Otud7a*-null mice had significant delay in almost all the milestones measured, with the exception of eye lid and ear opening (Figure 2B). However, there were no memory and learning deficits in adult *Otud7a*-null mice, as measured by fear conditioning and novel object recognition tests (Figures S1A–S1C).

All 15q13.3 homozygous microdeletion individuals and about 40% of heterozygous individuals have either a history of seizures or abnormal electrographic changes.[7] To evaluate the impact of *Otud7a* on brain activity, we recorded video-electroencephalography (EEG) and electromyography (EMG) in freely moving mice. We observed abnormal repetitive-spike events in all of the three male and three female *Otud7a*-null mice but not in any of the three male and three female wild-type littermates (Figures 3A and 3B; Table 2). Furthermore, we observed seizure-like events associated with behavioral arrest (see Movie S1 for example) in three out of six *Otud7a*-null mice, but not in any of the wild-types littermates (Figures 3C–3E; Table 2). Interestingly, instead of a generalized excessive or synchronous electrical discharge in the entire brain, these epileptiform activities were more prominent in the frontal cortex than the parietal cortex (Figures 3C–3E).

Language disability has been reported in all 15q13.3 homozygous microdeletion individuals and about 30% of heterozygous individuals.[7] In equivalence, we characterized ultrasonic vocalizations in pups of all three genotypes on postnatal day 2, 4, 6, 8, and 10, which was frequently used to assess vocalization and communication in rodents.[17–19] We found that mutant mice had an impairment in an *Otud7a* dosage-dependent manner, which was significant on day 8 (Figure 2C). Given that a subset of 15q13.3 microdeletion individuals have been diagnosed with autism spectrum disorder, which typically features social communication deficits, repetitive behaviors, and restricted interests, we also assessed social interaction and repetitive behaviors in *Otud7a* mice (Table 1). Results from these assays suggest that *Otud7a* deficiency leads to various differences in social behaviors in mice, which may or may not indicate autistic-like behaviors (Figures S1D–S1I).

Because all homozygous 15q13.3 microdeletion individuals reported in the literature had hypotonia and were non-ambulatory, we tested *Otud7a* mice for open field activity, grip strength, and performance on a rotating rod. We found that *Otud7a*-null mice were not significantly different from wild-type littermates in the distance traveled in the open field assay (Figure S1M). However, *Otud7a*-null mice had significantly reduced grip strength compared to their wild-type littermates (Figure 2D). Furthermore, *Otud7a*-null mice showed significant impairment in rotarod performance (Figures 2E and 2F), which suggests a deficit in motor coordination and motor learning.

Other neuropsychiatric and behavioral phenotypes, including attention deficit and hyperactivity disorder (ADHD), anxiety, and depression, have occasionally been reported in 15q13.3 microdeletion individuals. *Otud7a*-null mice did not show any significant differences from their wild-type littermates in any of the relevant assays that test for these conditions (Figures S1J–S1N). However,

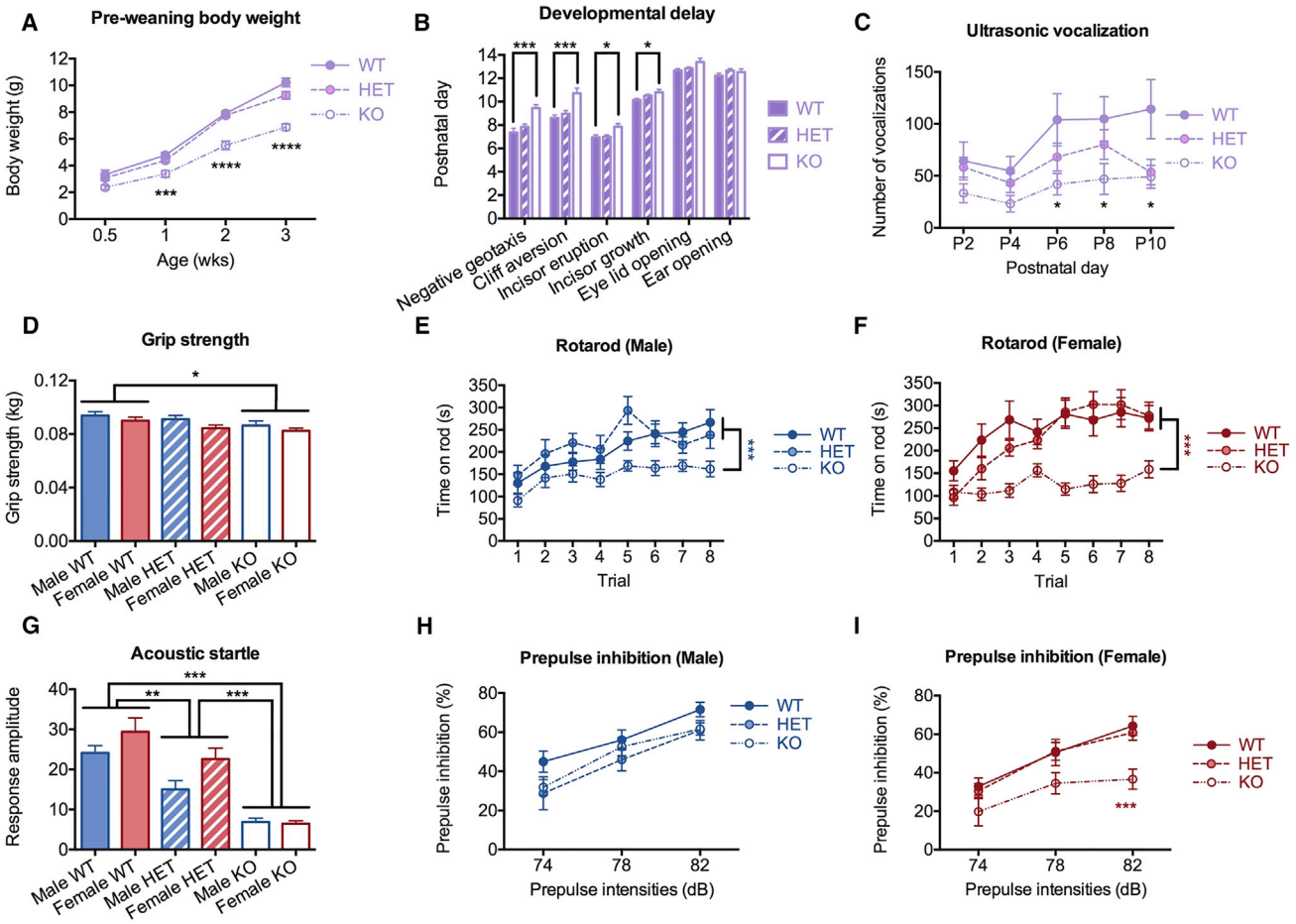

Figure 2. Mice Deficient in *Otud7a* Show Cardinal Phenotypes Related to 15q13.3 Microdeletion Syndrome
Data from male and female mice were combined for behavioral tests performed during pre-weaning period and were shown as bars or lines in purple. Behavioral data from male and female adult mice were shown separately, with males in blue and females in red.
(A) Null mice have decreased body weight prior to weaning.
(B) Null mice show developmental delay.
(C) Null mice show impaired ultrasonic vocalization.
(D) Null mice have reduced grip strength.
(E and F) Both male and female null mice show impairment in rotarod performance.
(G) Homozygous and heterozygous *Otud7a* knockout mice show reduced acoustic startle response.
(H and I) Male (H) and female (I) null mice manifest deficits in prepulse inhibition.
Data are presented as mean ± SEM (*$p < 0.05$, **$p < 0.01$, ***$p < 0.001$, ****$p < 0.0001$).

when we measured sensorimotor gating, a feature impaired in schizophrenia that has also been reported in 15q13.3 microdeletion individuals, we found that both homozygous and heterozygous *Otud7a* knockout mice had impaired acoustic startle response (Figure 2G). Additionally, female *Otud7a* homozygous null mice showed reduced prepulse inhibition at 82 dB prepulse intensity (Figure 2H). We tested hearing abilities of male and female *Otud7a* mutant mice using auditory brainstem response (ABR) and distortion product otoacoustic emissions (DPOAE) tests. We found that *Otud7a* mutant mice had no significant hearing loss at the age when they were tested for prepulse inhibition (Figure S2). These data suggest that female *Otud7a*-null mice have sensory-gating deficits.

One of the main questions regarding 15q13.3 microdeletion syndrome relates to the contribution of individual genes within the locus to the overall clinical phenotype. We therefore compared the phenotypes of our *Otud7a*-null mice with the established 15q13 microdeletion mouse model ($Df(h15q13)^{-/-}$), which had a deletion encompassing all six genes[20] (Table 3). The only behavioral abnormality present in the microdeletion mouse model that was not present in *Otud7a*-null mice is a learning and memory deficit. Otherwise, *Otud7a*-null mice recapitulated the cardinal phenotypes of the 15q13 deletion mouse as well as the main clinical aspects of the human microdeletion syndrome.

Role of Otud7a in Regulation of Dendritic Spine Density and Activity

Next, we began to investigate the cellular and molecular functions of *OTUD7A*, which were largely unknown.

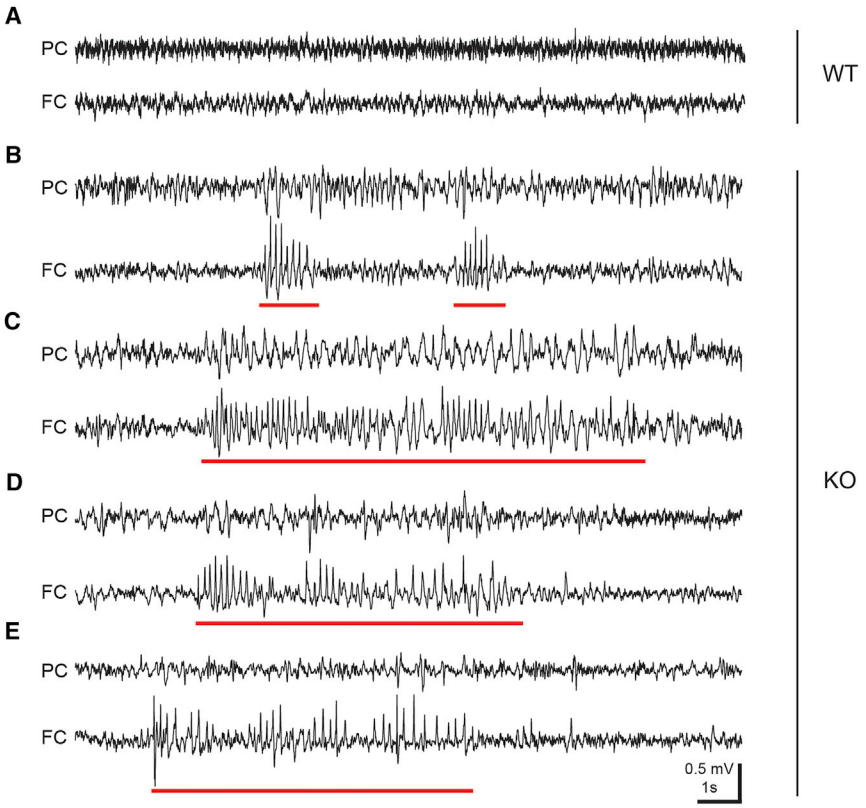

Figure 3. Abnormal EEG and Epileptiform Activities in *Otud7a*-Null Mice
Representative EEG traces from the parietal and frontal cortices of one WT (A) and four different null (B–E) mice. Red lines indicate the abnormal repetitive-spike events (B) or seizure-like events manifesting phenotypically as behavioral arrest (C–E). The seizure-like events lasted for 9.11 ± 0.98 s. The spike amplitude and frequency were 0.42 ± 0.02 mV and 4.77 ± 0.22 Hz, respectively. The data were obtained from 23 events in 3 mice and presented as mean ± SEM. Note, the data were also presented in Table 2 for each mouse. Abbreviations: PC, parietal cortex; FC, frontal cortex.

A published RNA-seq transcriptome database of different cell types in mouse cerebral cortexes showed that *Otud7a* has a relatively higher expression in neurons and oligodendrodyte progenitor cells compared to other cell types in the central nervous system.[21] Due to a lack of Otud7a-specific antibodies, we investigated the localization of N-terminally FLAG-tagged OTUD7A in mouse primary cortical neurons and observed an enrichment of OTUD7A at dendritic spines and membrane compartments in the cell body. Membrane localization of OTUD7A was also observed with a different construct expressing C-terminally Myc-FLAG tagged OTUD7A in HeLa cells (Figure S3), which is in contrast to the reported cytoplasmic localization of its homolog OTUD7B.[22] The reason for the differing localization of the two homologs may be the presence of lipid modification sites in OTUD7A, which are not present in OTUD7B (Table S2).

The distinct localization at dendritic spines suggests a potential role of OTUD7A in the regulation of synaptogenesis and synaptic plasticity. Therefore, we compared the number of spines in primary cortical neurons from *Otud7a*-null mice to those of their wild-type littermates, which revealed a significant reduction in spine density in the null mice (Figure 4B). The reduction of dendritic spine density in primary neurons from null mice was rescued by overexpressing OTUD7A (Figure 4B), which supports the notion that the phenotypes in *Otud7a* knockout mice were due to loss of OTUD7A function rather than a potential dominant-negative effect.

Enlightened by a companion manuscript in this issue of *AJHG* that utilizes a complementary approach to study *OTUD7A*,[23] we also examined its role in dendritic morphology of primary neurons. No significant difference in dendritic complexity was observed using Sholl analysis between primary cortical neurons from *Otud7a*-null mice and their wild-type littermates. However, overexpression of *Otud7a* led to significantly increased dendritic arborizations (Figure S4).

We performed Golgi-Cox staining of various cortical regions from *Otud7a*-null mice and wild-type littermates to investigate whether dendritic spine density was also decreased *in vivo*. We found that *Otud7a*-null mice had a decreased number of dendritic spines in the frontal cortex and motor cortex but not in the somatosensory cortex (Figure 5A), which was in line with observations in 15q13.3 microdeletion mice.[23] To determine whether decreased spine density may lead to an impairment in glutamatergic synaptic transmission, we performed whole-cell recording of miniature excitatory postsynaptic currents (mEPSCs) in frontal cortices of *Otud7a*-null and wild-type littermates. We found a reduction in the frequency of mEPSCs in knockout mice, while the amplitude of mEPSCs was unchanged (Figure 5B). Taken together, the decreased dendritic spine density and the decreased mEPSC frequency indicates that *Otud7a* deficiency reduces the number of functioning excitatory synapses.

Discussion

In summary, our results show that *Otud7a* heterozygous and homozygous knockout mice have recapitulated cardinal phenotypes associated with 15q13.3 microdeletion syndrome. Heterozygous mice show reduced ultrasonic vocalization and acoustic startle deficit, and homozygous knockout mice recapitulate developmental delay, vocal

Table 2. Quantification of Repetitive-Spike Events and Seizure-like Events

Mouse ID	Genotype	Rate of Repetitive-Spike Events (#/hour)	Number of Seizure-like Events	Rate of Seizure-like Events (#/hour)	Duration of Seizure-like Events (s)	Spike Amplitude in Seizure-like Events (mV)	Spike Frequency in Seizure-like Events (Hz)
C371	KO	20.63	4	0.50	7.91 ± 0.22	0.32 ± 0.01	4.79 ± 0.13
C372	KO	5.62	0	0	N/A	N/A	N/A
C374	KO	11.38	0	0	N/A	N/A	N/A
C375	KO	59.37	15	1.88	9.35 ± 1.47	0.47 ± 0.03	4.39 ± 0.22
C399	KO	1.00	0	0	N/A	N/A	N/A
C400	KO	0.83	4	0.67	9.42 ± 1.43	0.35 ± 0.01	6.19 ± 0.50

No repetitive-spike events or seizure-like events was observed in wild-type littermates.

impairment, seizure-related abnormalities, motor deficits, hypotonia, and acoustic startle deficit. It is not uncommon to see that mouse neurobehavioral phenotypes are milder when compared with humans. For several human disorders that are pathogenic in heterozygous state, the mouse model is not or is barely significant in heterozygous state, but is convincingly significant in homozygous state. Examples include *SHANK3* for Phelan-McDermid syndrome,[24] *RAI1* for Smith-Magenis syndrome,[25] and *MECP2* in females for Rett syndrome.[26]

Our results, together with findings from the companion manuscript,[23] suggest that *OTUD7A* deficiency largely accounts for phenotypes associated with 15q13.3 microdeletion syndrome and that *OTUD7A* is important in regulation of dendritic spine density and activity. Our finding that *OTUD7A* is crucial for the development and functioning of central nervous system is also well supported by a pLI (probability of loss-of-function intolerance) score of 0.97 in the ExAC database. In ExAC, loss-of-function variants were found at a rate of 1 in every 10,223 individuals enrolled in their study of presumably unaffected individuals. Detailed neuropsychiatric phenotypic information is not available for those individuals. The development of therapeutic intervention for 15q13.3 microdeletion syndrome should take OTUD7A haploinsufficiency into consideration, and future work should

Table 3. Comparison of Behavioral and Electrophysiological Phenotypes between 15q13.3 Homozygous Knockout Mice and *Otud7a*-Null Mice

Phenotypes/Behavioral Assays	*Df(h15q13)*$^{-/-}$	*Otud7a*$^{-/-}$
Body weight	decreased	decreased
Ultrasonic vocalization	impaired	impaired
Acoustic startle	impaired	impaired
Prepulse inhibition	impaired	impaired
Grip strength	decreased	decreased in female, trend toward decrease in male
Seizures/EEG recording	altered seizure response to PTZ administration	spontaneous EEG abnormalities
Open field	no significant change	no significant change
Three-chamber test	no impairment	no impairment
Developmental delay	not assessed	developmental delay
Rotarod performance	not assessed	impaired
Elevated plus maze	not assessed	no significant change
Novel object recognition	not assessed	no significant change
Forced swimming	not assessed	no significant change
Partition test	not assessed	no impairment
Morris water maze	inconclusive due to vision impairment	not assessed due to motor deficits
Nest building[a]	impaired	trend toward impairment but no significant change
Fear conditioning	decreased cued fear memory	no significant change in female, increased cued fear memory in male

Reference for behavioral phenotypes in *Df(h15q13)*$^{-/-}$ mice: Forsingdal et al.[20]
[a]In the *Df(h15q13)*$^{-/-}$ study, 6 knockout mice with mixed gender were assessed. In our study, 14 male *Otud7a*$^{-/-}$ mice and 16 female *Otud7a*$^{-/-}$ mice were assessed.

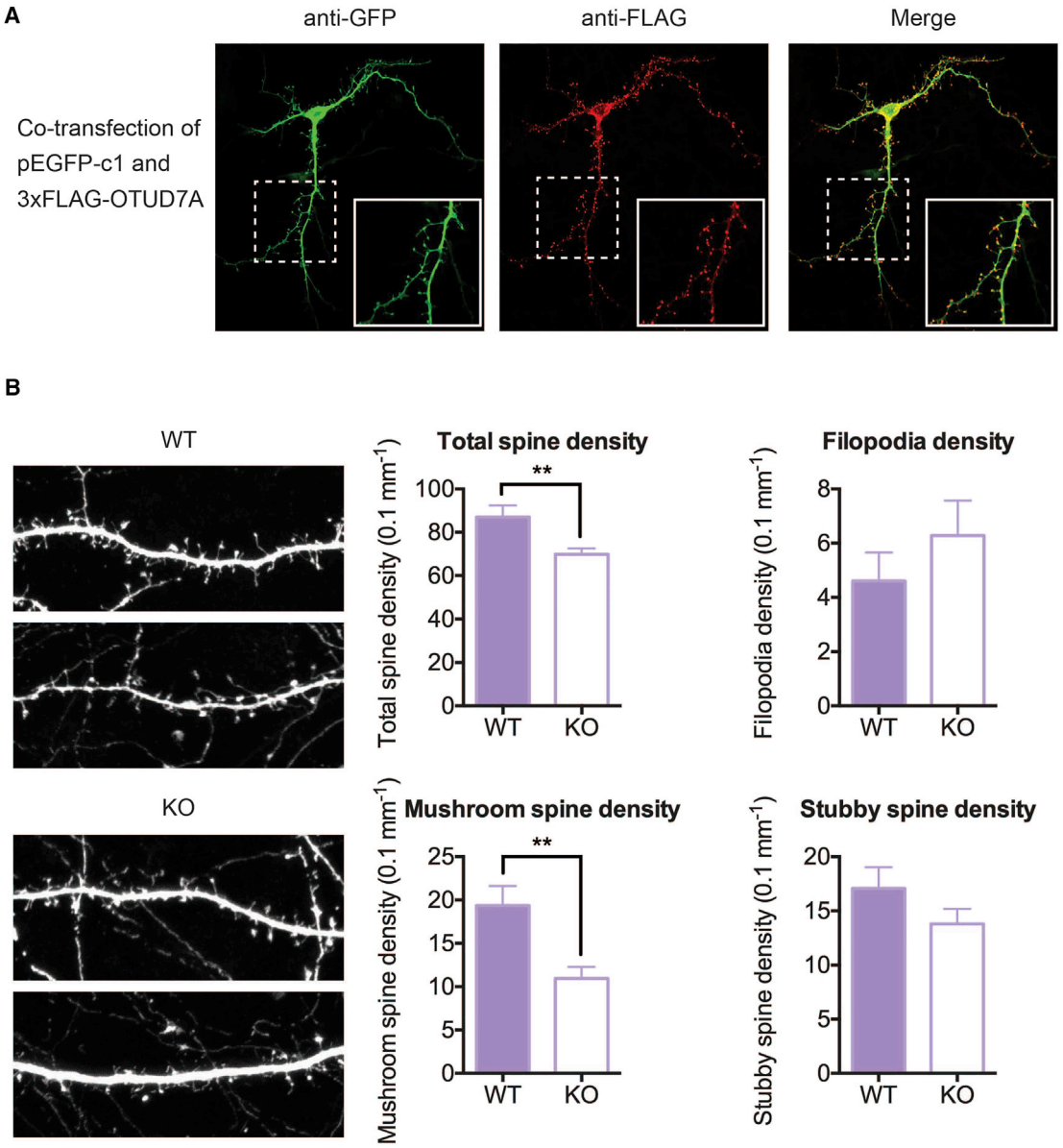

Figure 4. OTUD7A Localizes to Dendritic Spines and Regulates Spine Density

(A) OTUD7A localizes to dendritic spines. Mouse primary cortical cultures were co-transfected with pEGFP-c1 and 3xFLAG-OTUD7A on DIV 7. On DIV 14, immunofluorescent imaging was performed, with GFP in green (Alexa488) and FLAG in red (Cy3). The bottom right corner of each image shows a magnification of the inset box.

(B) Primary cortical neurons from *Otud7a*-null mice show decreased total spine density compared to wild-type neurons, which are rescued by overexpression of *Otud7a*. To compare between genotypes, primary cortical neurons from *Otud7a*-null mice or wild-type littermates were transfected with pEGFP-c1 and stained with GFP antibody. As a rescue experiment, primary neurons from *Otud7a*-null mice were transfected with 700 ng 3xFLAG-OTUD7A per 24-well. We investigated 42 neurons/dendrites from 9 null mice, 41 neurons/dendrites from 3 wild-type mice, and 31 neurons/dendrites from 9 null mice in the rescue experiments. Top: representative examples of dendritic segments of the immune-stained neurons. Bottom: quantification of dendritic spines. Statistical significance was assessed using two-tailed t test. Data are presented as mean ± SEM (*$p < 0.05$, **$p < 0.01$, ***$p < 0.001$).

involve the investigation of molecular pathways regulated by OTUD7A.

Given that cognitive and social deficits were not observed in *Otud7a* knockout mice, genetic background or other genes associated with the deletions may complement and interact with *Otud7a* to contribute to disease manifestation. Future investigations may involve (1) an assessment of the consequences of *Otud7a* loss of function in mice of various genetic backgrounds, (2) rescuing 15q13.3 homozygous knockout mice with transgenes expressing *Chrna7* or *Otud7a*, or (3) the generation of mice with deletion of both *Chrna7* and *Otud7a*.

We observed no dendrite growth defects in *Otud7a* homozygous knockout mice, while 15q13.3 microdeletion mice had decreased cortical neuron dendritic complexity.[23] This indicates that *Otud7a* is not necessary for

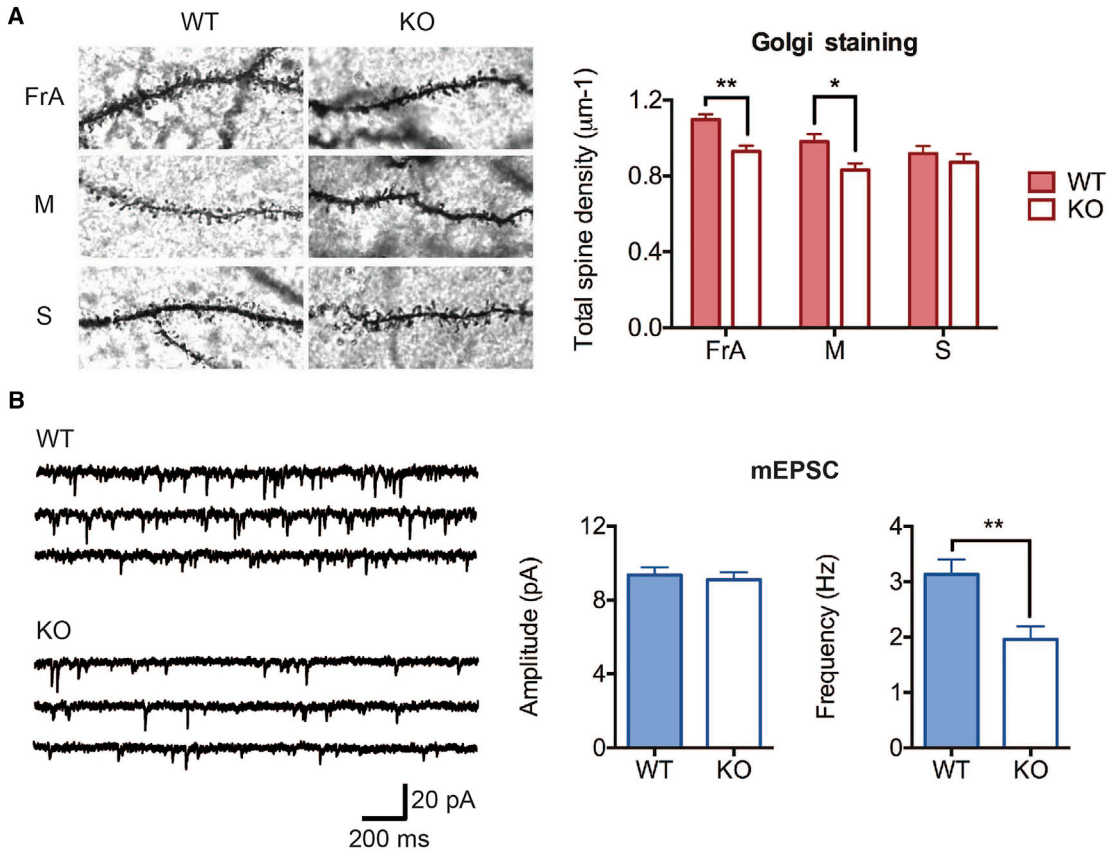

Figure 5. *Otud7a*-Null Mice Display Significantly Reduced Number of Functioning Excitatory Synapses
(A) Golgi-Cox staining shows significantly reduced number of dendritic spines in the frontal association cortex (FrA) and motor cortex (M) but not in the somatosensory cortex (S). Data were obtained from basal dendrites of layer II/III pyramidal neurons (n = 16–20) from 3 null and 3 wild-type female mice at 4 weeks old. Left: representative examples of dendritic segments of the Golgi-Cox stained neurons. Right: quantification of dendritic spine densities.
(B) *Otud7a*-null mice display significantly reduced mEPSC frequency in frontal cortices. Left: sample traces of mEPSCs. Right: average of amplitude and frequency of mEPSCs. Whole-cell recordings were performed on layer II/III pyramidal neurons from four null (n = 11) and four wild-type (n = 15) male mice at 8 to 11 weeks old. Data are presented as mean ± SEM (*p < 0.05, **p < 0.01).

dendritic growth. However, the fact that overexpression of *Otud7a* significantly promoted dendritic arborization and that the dendritic growth defects in neurons from 15q13.3 microdeletion mice were rescued by overexpression of either *Otud7a* or *Chrna7*[23] suggest that *Otud7a* has the capacity to regulate dendritic growth.

Some groups claimed to have identified small deletions in individuals that encompass only *CHRNA7*,[8,16,27] but we found that several of the reported deletions affected also the first exon of *OTUD7A*. In the article by Liao et al.,[3] array CGH identified a deletion that included part of *OTUD7A*, although the undeleted region of *OTUD7A* seemed to be adequate for binding of a bacterial artificial chromosome (BAC) FISH probe. The same is true for the article by Masurel-Paulet et al.:[16] part of *OTUD7A* were involved in the smallest deletions. In the article by Prasun et al.,[28] the lack of coverage at the 5′ region of *OTUD7A* prevented to assess its possible rearrangement. The first exon of *OTUD7A* locates in a segmental duplication and is thus susceptible to chromosome rearrangements. The deletion of the first exon or 5′ region could obviously affect regulation and expression of the respective gene. Analysis of *OTUD7A* mRNA expression in cell lines generated from the affected individuals with small deletions would be necessary to further investigate the consequences of the respective genomic deletions.

Supplemental Data

Supplemental Data include four figures, three tables, and one movie and can be found with this article online at https://doi.org/10.1016/j.ajhg.2018.01.005.

Acknowledgments

The work was supported in part by the BCM Intellectual and Developmental Disabilities Research Center Neuroconnectivity, Neurovisualization and Neurobehavioral Cores (NIH grant U54HD083092), the BCM Genetically Engineered Mouse Core (NIH grants P30CA125123, U42HG006352), NIH grant DP5OD009134 (R.C.S.), NIH grant R01NS100893 (M.X.), the Whitehall Foundation (M.X.), and Citizens United for Research in Epilepsy (M.X.). M.X. is a Caroline DeLuca Scholar. C.P.S. is generously supported by the Joan and Stanford Alexander Family. Video EEG recordings were performed by Zhenyu Wu and

Dr. Jianrong Tang at the Neuroconnectivity Core and In Vivo Neurophysiology Core and Golgi-Cox staining was performed by Tao Lin at the Neuropathology Core of Jan and Dan Duncan Neurological Research Institute.

Received: September 6, 2017
Accepted: January 10, 2018
Published: February 1, 2018

Web Resource

CRISPR design tool, http://crispr.mit.edu/
dbGaP (phs000424.v7.p2), http://www.ncbi.nlm.nih.gov/gap
ExAC Browser, http://exac.broadinstitute.org/gene/ENSG00000169918
GTEx Portal, https://www.gtexportal.org/home/gene/OTUD7A
OMIM, http://www.omim.org/

References

1. Sharp, A.J., Mefford, H.C., Li, K., Baker, C., Skinner, C., Stevenson, R.E., Schroer, R.J., Novara, F., De Gregori, M., Ciccone, R., et al. (2008). A recurrent 15q13.3 microdeletion syndrome associated with mental retardation and seizures. Nat. Genet. *40*, 322–328.
2. van Bon, B.W.M., Mefford, H.C., Menten, B., Koolen, D.A., Sharp, A.J., Nillesen, W.M., Innis, J.W., de Ravel, T.J.L., Mercer, C.L., Fichera, M., et al. (2009). Further delineation of the 15q13 microdeletion and duplication syndromes: a clinical spectrum varying from non-pathogenic to a severe outcome. J. Med. Genet. *46*, 511–523.
3. Liao, J., DeWard, S.J., Madan-Khetarpal, S., Surti, U., and Hu, J. (2011). A small homozygous microdeletion of 15q13.3 including the CHRNA7 gene in a girl with a spectrum of severe neurodevelopmental features. Am. J. Med. Genet. A. *155A*, 2795–2800.
4. Lepichon, J.-B., Bittel, D.C., Graf, W.D., and Yu, S. (2010). A 15q13.3 homozygous microdeletion associated with a severe neurodevelopmental disorder suggests putative functions of the TRPM1, CHRNA7, and other homozygously deleted genes. Am. J. Med. Genet. A. *152A*, 1300–1304.
5. Shinawi, M., Schaaf, C.P., Bhatt, S.S., Xia, Z., Patel, A., Cheung, S.W., Lanpher, B., Nagl, S., Herding, H.S., Nevinny-Stickel, C., et al. (2009). A small recurrent deletion within 15q13.3 is associated with a range of neurodevelopmental phenotypes. Nat. Genet. *41*, 1269–1271.
6. Lowther, C., Costain, G., Stavropoulos, D.J., Melvin, R., Silversides, C.K., Andrade, D.M., So, J., Faghfoury, H., Lionel, A.C., Marshall, C.R., et al. (2015). Delineating the 15q13.3 microdeletion phenotype: a case series and comprehensive review of the literature. Genet. Med. *17*, 149–157.
7. Gillentine, M.A., and Schaaf, C.P. (2015). The human clinical phenotypes of altered CHRNA7 copy number. Biochem. Pharmacol. *97*, 352–362.
8. Hoppman-Chaney, N., Wain, K., Seger, P.R., Superneau, D.W., and Hodge, J.C. (2013). Identification of single gene deletions at 15q13.3: further evidence that CHRNA7 causes the 15q13.3 microdeletion syndrome phenotype. Clin. Genet. *83*, 345–351.
9. Yin, J., Chen, W., Yang, H., Xue, M., and Schaaf, C.P. (2017). Chrna7 deficient mice manifest no consistent neuropsychiatric and behavioral phenotypes. Sci. Rep. *7*, 39941.
10. Fotaki, V., Dierssen, M., Alcántara, S., Martínez, S., Martí, E., Casas, C., Visa, J., Soriano, E., Estivill, X., and Arbonés, M.L. (2002). Dyrk1A haploinsufficiency affects viability and causes developmental delay and abnormal brain morphology in mice. Mol. Cell. Biol. *22*, 6636–6647.
12. Hao, S., Tang, B., Wu, Z., Ure, K., Sun, Y., Tao, H., Gao, Y., Patel, A.J., Curry, D.J., Samaco, R.C., et al. (2015). Forniceal deep brain stimulation rescues hippocampal memory in Rett syndrome mice. Nature *526*, 430–434.
13. Parnass, Z., Tashiro, A., and Yuste, R. (2000). Analysis of spine morphological plasticity in developing hippocampal pyramidal neurons. Hippocampus *10*, 561–568.
14. Spielmann, M., Reichelt, G., Hertzberg, C., Trimborn, M., Mundlos, S., Horn, D., and Klopocki, E. (2011). Homozygous deletion of chromosome 15q13.3 including CHRNA7 causes severe mental retardation, seizures, muscular hypotonia, and the loss of KLF13 and TRPM1 potentially cause macrocytosis and congenital retinal dysfunction in siblings. Eur. J. Med. Genet. *54*, e441–e445.
15. Endris, V., Hackmann, K., Neuhann, T.M., Grasshoff, U., Bonin, M., Haug, U., Hahn, G., Schallner, J.C., Schröck, E., Tinschert, S., et al. (2010). Homozygous loss of CHRNA7 on chromosome 15q13.3 causes severe encephalopathy with seizures and hypotonia. Am. J. Med. Genet. A. *152A*, 2908–2911.
16. Masurel-Paulet, A., Andrieux, J., Callier, P., Cuisset, J.M., Le Caignec, C., Holder, M., Thauvin-Robinet, C., Doray, B., Flori, E., Alex-Cordier, M.P., et al. (2010). Delineation of 15q13.3 microdeletions. Clin. Genet. *78*, 149–161.
17. Shu, W., Cho, J.Y., Jiang, Y., Zhang, M., Weisz, D., Elder, G.A., Schmeidler, J., De Gasperi, R., Sosa, M.A.G., Rabidou, D., et al. (2005). Altered ultrasonic vocalization in mice with a disruption in the Foxp2 gene. Proc. Natl. Acad. Sci. USA *102*, 9643–9648.
18. Scattoni, M.L., Crawley, J., and Ricceri, L. (2009). Ultrasonic vocalizations: a tool for behavioural phenotyping of mouse models of neurodevelopmental disorders. Neurosci. Biobehav. Rev. *33*, 508–515.
19. Peñagarikano, O., Abrahams, B.S., Herman, E.I., Winden, K.D., Gdalyahu, A., Dong, H., Sonnenblick, L.I., Gruver, R., Almajano, J., Bragin, A., et al. (2011). Absence of CNTNAP2 leads to epilepsy, neuronal migration abnormalities, and core autism-related deficits. Cell *147*, 235–246.
20. Forsingdal, A., Fejgin, K., Nielsen, V., Werge, T., and Nielsen, J. (2016). 15q13.3 homozygous knockout mouse model display epilepsy-, autism- and schizophrenia-related phenotypes. Transl. Psychiatry *6*, e860.
21. Zhang, Y., Chen, K., Sloan, S.A., Bennett, M.L., Scholze, A.R., O'Keeffe, S., Phatnani, H.P., Guarnieri, P., Caneda, C., Ruderisch, N., et al. (2014). An RNA-sequencing transcriptome and splicing database of glia, neurons, and vascular cells of the cerebral cortex. J. Neurosci. *34*, 11929–11947.
22. Urbé, S., Liu, H., Hayes, S.D., Heride, C., Rigden, D.J., and Clague, M.J. (2012). Systematic survey of deubiquitinase localization identifies USP21 as a regulator of centrosome- and microtubule-associated functions. Mol. Biol. Cell *23*, 1095–1103.
23. Uddin, M., Unda, B.K., Kwan, V., Holzapfel, N.T., White, S.H., Chalil, L., Woodbury-Smith, M., Ho, K.S., Harward, E., Murtaza, N., et al. (2018). OTUD7A regulates neurodevelopmental phenotypes in the 15q13.3 microdeletion syndrome. Am. J. Hum. Genet. *102*, this issue, 278–295.

24. Drapeau, E., Dorr, N.P., Elder, G.A., and Buxbaum, J.D. (2014). Absence of strong strain effects in behavioral analyses of Shank3-deficient mice. Dis. Model. Mech. *7*, 667–681.
25. Bi, W., Ohyama, T., Nakamura, H., Yan, J., Visvanathan, J., Justice, M.J., and Lupski, J.R. (2005). Inactivation of Rai1 in mice recapitulates phenotypes observed in chromosome engineered mouse models for Smith-Magenis syndrome. Hum. Mol. Genet. *14*, 983–995.
26. Guy, J., Hendrich, B., Holmes, M., Martin, J.E., and Bird, A. (2001). A mouse Mecp2-null mutation causes neurological symptoms that mimic Rett syndrome. Nat. Genet. *27*, 322–326.
27. Mikhail, F.M., Lose, E.J., Robin, N.H., Descartes, M.D., Rutledge, K.D., Rutledge, S.L., Korf, B.R., and Carroll, A.J. (2011). Clinically relevant single gene or intragenic deletions encompassing critical neurodevelopmental genes in patients with developmental delay, mental retardation, and/or autism spectrum disorders. Am. J. Med. Genet. A. *155A*, 2386–2396.
28. Prasun, P., Hankerd, M., Kristofice, M., Scussel, L., Sivaswamy, L., and Ebrahim, S. (2014). Compound heterozygous microdeletion of chromosome 15q13.3 region in a child with hypotonia, impaired vision, and global developmental delay. Am. J. Med. Genet. A. *164A*, 1815–1820.